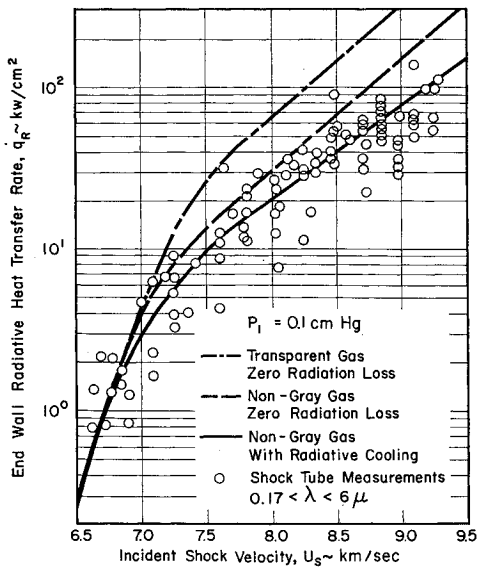

Fig. 2 Comparison of shock tube end-wall radiative heat-transfer rate measurements with calculations using five-step absorption coefficient model.

lated values obtained by using the present five-step absorption coefficient model in the numerical solution of Ref. 7 are also shown in this figure and reasonable agreement is seen to exist. This favorable comparison may be contrasted with that provided by the other two calculations shown in Fig. 2. The first is for an isothermal transparent slab (no radiative cooling or self-absorption), and the second includes only self-absorption (without radiative cooling). As may be seen, for the higher velocities the former is a factor of three and the latter approximately 50% greater than the mean of the data. It is only at the lowest velocities that these three calculations are in agreement. Thus, the effects of self-absorption and radiative cooling both appear to be important for the present conditions. Although the calculations shown in Fig. 2 suggest that self-absorption is the more important of these two effects, photomultiplier measurements of the radiative time-history behind reflected shock waves in air at these conditions indicate that significant radiative cooling is also present.

It should be noted that the present calculations are as much as 25–50% lower than the earlier two-step model calculations of Ref. 1, and are in reasonable agreement with the mean of the data. It should also be noted that a similar absorption coefficient model has been used by Page et al.[8] in carrying out theoretical calculations of stagnation-point radiative heat transfer at super-orbital velocities. Because of the similarities between the absorption coefficient models, the present agreement with experiment indirectly supports the calculations of Page et al.

References

[1] Golobic, R. A. and Nerem, R.M., "Shock Tube Measurements of End-Wall Radiative Heat Transfer in Air," *AIAA Journal*, Vol. 6, No. 9, Sept. 1968, pp. 1741–1747.

[2] Weise, W. L., Smith, M. W., and Glennon, B. M., "Atomic Line Transition Probabilities, Hydrogen Through Neon," Vol. 1, NBS Rept. NSRDS-NBS4, May 1966, National Bureau of Standards.

[3] Wilson, K. W. and Nicolet, W. E., "Spectral Absorption Coefficients of Carbon, Nitrogen, and Oxygen Atoms," Rept. 4-17-66-5, Nov. 1965, Lockheed Missiles & Space Co., Palo Alto, Calif.

[4] Armstrong, B. H., "Apparent Positions of Photoelectric Edges and the Merging of Spectral Lines," *Journal of Quantitative Spectroscopy & Radiative Transfer*, Vol. 4, 1964, pp. 207–214.

[5] Nerem, R. M. and Stickford, G. H., "Shock Tube Studies of Equilibrium Air Radiation," *AIAA Journal*, Vol. 3, No. 6, June 1965, pp. 1011–1018.

[6] Wilson, K. H., private communication, 1967, Lockheed Palo Alto Research Lab.

[7] Anderson, J. D., "Radiative Transfer Effects on the Flow Field and Heat Transfer Behind a Reflected Shock Wave in Air," *The Physics of Fluids*, Vol. 10, No. 8, Aug. 1967, pp. 1785–1793.

[8] Page, W. A. et al., "Radiative Transport in Inviscid Non-adiabatic Stagnation-Region Shock Layers," AIAA Paper 68-784, Los Angeles, Calif., 1968.

Thermal Transport and Relaxation Processes in Shock-Heated Argon

KLAUS WILLEKE* AND DANIEL BERSHADER†
Stanford University, Stanford, Calif.

THIS Note reports the results of experiments on high-temperature thermal transport and ionization relaxation in argon. The measurements were made with an improved thin-film surface thermometer[1] located in the end wall of the Stanford Aerophysics Laboratory high-pressure shock tube and were intended to constitute an independent check on similar studies made by the optical interferometric technique.[2] Measurement of temperature as a function of time following shock reflection yielded heat-transfer rates from the wall thermal layer in a temperature range not attained previously with this type of device.

The resistance thermometer heat gage consists of a triple-layered element (40 Å Cr–400 Å Pt–400 Å Cr) coated by a somewhat thicker layer of SiO_2 (8000 Å). The coating is chemically matched to the quartz (SiO_2) substrate such that the sensor is embedded essentially in a homogeneous medium. Its response to a heat input at the gage surface is then obtainable by means of a simple transfer function.

Figure 1 shows the heat-gage response in argon. The first rise occurs upon shock reflection from the end wall and is caused by the sudden deposition of energy into the translational mode of the gas. All internal degrees of freedom are "frozen" for some time, typically a few microseconds for present experimental conditions. Equilibrium ionization is attained at the end of a characteristic relaxation time. The latter stages of the approach to equilibrium are quite rapid. Consequent modification of the thermochemical state of the gas produces a corresponding effect on the thermal transport and, therefore, on the wall temperature behavior. The latter change is seen as the second rise in Fig. 1. That figure, therefore, contains information on 1) heat transfer from the non-ionized gas at "frozen" temperatures in excess of 1 ev, 2) re-

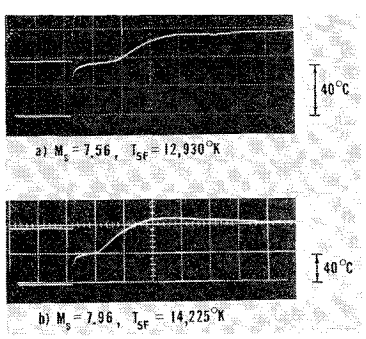

Fig. 1 Response of end-wall heat-transfer gage in argon; P_1 = 10 torr, T_1 = 297°K, sweep speed = 50 μsec/div; T_{5F} represents "frozen" temperature of the non-ionized gas behind the reflected shock.

Received June 23, 1969. This work was supported by NASA Grant NGR-05-020-091.

* Research Fellow; presently Postdoctoral Fellow at the Institut für Plasmaphysik, Garching bei München, West Germany. Member AIAA.

† Professor of Aerophysics and Associate Chairman, Department of Aeronautics and Astronautics. Associate Fellow AIAA.

laxation time to ionization, and 3) additional heat transfer associated with the appearance of substantial numbers of electrons at or near the end of the ionization relaxation process.

We have deduced the thermal conductivity dependence on temperature for "frozen" argon over the temperature range of 2100° to 16,400°K by minimizing the root-mean-square deviation between the experimental traces and theoretical gage responses calculated numerically by the use of the usual boundary-layer equations and the thermal conductivity expression

$$\varkappa = \varkappa_0(T/T_0)^\nu \tag{1}$$

The form for $\varkappa$ given by Eq. (1) stems from kinetic theory, where the interatomic potential is taken as proportional to an inverse power of the separation. The potential is predominantly repulsive at higher temperatures. The analysis by Amdur and Mason,[3] who used somewhat more complex potential functions deduced from atomic-beam scattering experiments, showed a good fit with Eq. (1) for $\nu = 0.75$ for the case of nonionized argon.

In the present study, ten experiments were evaluated and gave

$$\nu = 0.749 \pm 0.023 \tag{2}$$

a result that confirms the Amdur-Mason prediction. The preceding value agrees, as well, with the work of Kuiper,[2] whose analysis, in turn, includes a corrected version of the experimental results reported by Bunting and Devoto.[4] In Kuiper's optical work, the measured quantity is the end-wall boundary-layer profile of density. The latter is converted to temperature and compared with a profile constructed from a theoretical boundary-layer analysis which involves the exponent ν as a parameter. Thus the two experimental studies are quite independent.

Figure 2 shows the present results expressed as a scaled heat flux vs Mach number in comparison with calculated predictions for various values of ν. The clustering of the points around the curve for $\nu = 0.75$ is consistent with the result indicated in Eq. (2).

Table 1 summarizes the results of several other investigations and includes ours as well. There is generally good agreement with respect to the value of ν, but note that Matula[6] and Collins and Menard[5] worked in rather restricted temperature ranges. Further, Camac and Feinberg,[7] who worked with a unique infrared-type gage, subsequently found a calibration error[8] that adds further uncertainty to their result. The temperature ranges in Table 1 indicate the freestream temperature of argon.

We turn now to the relaxation time studies. The rapid production of electrons in the gas outside the thermal layer near the termination of the relaxation processes is followed by a penetration of the same process into the layer itself. The presence of free charges has two effects on thermal transport.

Table 1 Values of power law exponent ν for thermal conductivity of argon: $\kappa/\kappa_w = (T/T_w)^\nu$

Amdur and Mason[3] (theoretical)	1,000°K < T < 15,000°K	$\nu = 0.75$
Collins and Menard[5] (surface resistance gage)	1,500°K < T < 5,000°K	$\nu = 0.703$
Matula[6] (surface resistance gage)	1,500°K < T < 4,800°K	$\nu = 0.68$
Camac and Feinberg[7] (surface IR gage)	20,000°K < T < 75,000°K	$\nu = 0.76$
Kuiper[2] (based on Bunting and Devoto[4]) (optical interferometry)	2,500°K < T < 9,200°K	$\nu = 0.75$
Present work[1] (surface resistance gage)	2,100°K < T < 16,400°K	$\nu = 0.75$

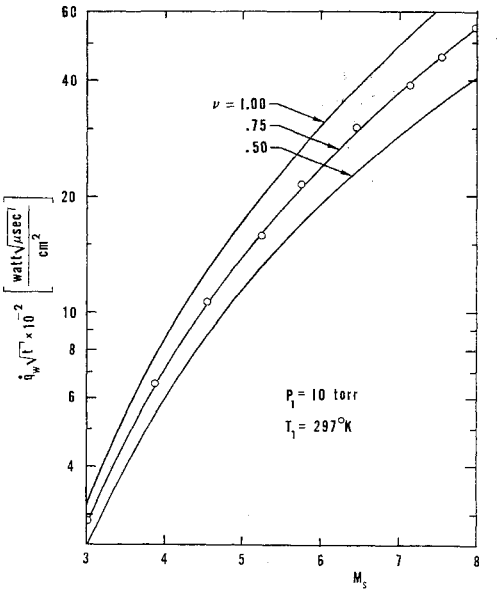

Fig. 2 Comparison of experimental (scaled) heat flux values in shock-heated argon with theoretical predictions for several values of the thermal conductivity power law parameter ν [$\kappa/\kappa_W = (T/T_W)^\nu$]. Graph shows heat flux vs Mach number of incident shock. Note that reflected shock temperature and density for the case $M_S = 8$ are, respectively, $T_{5F} = 14{,}400$°K and $\rho_{5F} = 2.02 \times 10^{-4}$ g/cm³.

Firstly, there is a modification of the temperature gradient and, therefore, of the Fourier conductivity. Balancing that change is the transport of chemical enthalpy by ambipolar diffusion, with recombination taking place both in the cooler parts of the boundary layer and at the wall. Secondly, there is a modification of the effective thermal conductivity due to the presence of free electrons. The result appears as a second rise in the temperature response curves of Fig. 1. This is the first time, to the authors' knowledge, that such measurements have been recorded by this type of gage. The time lapse between the two breaks in those curves corresponds to a relaxation time for ionization in the end-wall region. The times between shock reflection and the inflection point of the second rise were found to be in close agreement with Kuiper's[2] interferometric measurements of ionization times behind incident and reflected shock waves in argon. Figure 3 gives

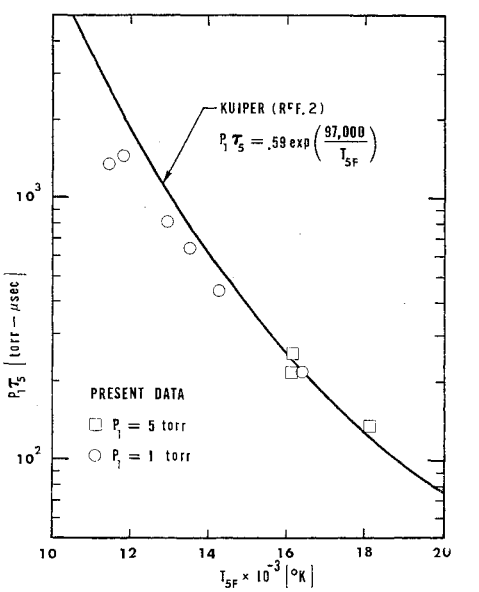

Fig. 3 Ionization-relaxation times behind reflected shocks in argon, measured by shock-tube end-wall heat gage.

the product of initial test-section pressure and ionization time as a function of reflected-shock-region temperature. It illustrates the close agreement between results obtained from Kuiper's interferometric measurements of the thermal boundary layer and those obtained from the present heat-gage measurements on the wall.

Measurements of the second rise show that ionization relaxation increases the thermal transport to the wall by a significant amount. For example, heat transfer was approximately doubled for the case of an incident-shock Mach number of 8 advancing into room-temperature argon at 10 torr pressure. The second rise of the heat-gage response levels off to a fairly constant value. That should permit some future deduction of thermal conductivity coefficients in ionized gases as well.

References

[1] Willeke, K., "Shock-Tube Study of the Transient Thermal Behavior of Gases at High Temperatures," SUDAAR 375, May 1969, Dept. of Aeronautics and Astronautics, Stanford Univ., Stanford, Calif.

[2] Kuiper, R. A., "Interferometric Study of the End-Wall Thermal Layer in Ionizing Argon," AIAA Paper 69-694, San Francisco, Calif., 1969.

[3] Amdur, I. and Mason, E. A., "Properties of Gases at Very High Temperatures," *The Physics of Fluids*, Vol. 1, No. 5, Sept. 1958, pp. 370–383.

[4] Bunting, J. O. and Devoto, R. S., "Shock-Tube Study of the Thermal Conductivity of Argon," SUDAAR 313, July 1967, Dept. of Aeronautics and Astronautics, Stanford Univ., Stanford, Calif.

[5] Collins, D. J. and Menard, W. A., "Measurement of the Thermal Conductivity of Noble Gases in the Temperature Range 1,500 to 5,000°K," *Journal of Heat Transfer*, Vol. 88, Feb. 1966, pp. 52–56.

[6] Matula, R. A., "High Temperature Thermal Conductivity of Rare Gases and Gas Mixtures," *Transactions of the ASME, Series C*, Vol. 90, No. 3, Aug. 1968, pp. 319–327.

[7] Camac, M. and Feinberg, R. M., "Thermal Conductivity of Argon at High Temperatures," *Journal of Fluid Mechanics*, Vol. 21, Pt. 4, April 1965, pp. 673–688.

[8] Fay, J. A. and Arnoldi, D., "High-Temperature Thermal Conductivity of Argon," *The Physics of Fluids*, Vol. 11, No. 5, May 1968, pp. 983–985.

Thermal Stresses in a Transversely Isotropic, Hollow, Circular Cylinder

D. B. Longcope,* M. J. Forrestal,† and W. E. Warren†

Sandia Laboratories, Albuquerque, N. Mex.

Introduction

FORMULAS for the thermal stresses in an isotropic, hollow, circular cylinder with a two-dimensional temperature distribution independent of the axial coordinate have been derived by Forray.[1–3] In this Note, formulas are developed for the thermal stresses in a transversely isotropic, hollow, circular cylinder. These results can be used to estimate thermal stresses in re-entry vehicles which arise from aerodynamic heating.

Statement of the Problem

Utilizing the static, linear theory of thermoelasticity for a state of plane strain, expressions are developed for the stress and displacement fields in a hollow, circular cylinder of inner radius a and outer radius b which is fabricated from a material exhibiting transverse isotropy along the radial direction. The cylinder is subjected to an arbitrary temperature distribution independent of the axial coordinate and the cylindrical surfaces are assumed stress free.

Under conditions of plane strain, the stress-displacement relations in cylindrical coordinates are

$$\sigma_r = c_{11}(\partial U/\partial R) + c_{12}[(U/R) + (\partial V/R\partial\theta)] - \lambda_1 T \quad (1a)$$

$$\sigma_\theta = c_{12}(\partial U/\partial R) + c_{22}[(U/R) + (\partial V/R\partial\theta)] - \lambda_2 T \quad (1b)$$

$$\sigma_z = c_{12}(\partial U/\partial R) + c_{23}[(U/R) + (\partial V/R\partial\theta)] - \lambda_2 T \quad (1c)$$

$$\tau_{r\theta} = c_{44}[(\partial U/R\partial\theta) + (\partial V/\partial R) - (V/R)] \quad (1d)$$

where

$$\lambda_1 = c_{11}\alpha_1 + 2c_{12}\alpha_2, \qquad \lambda_2 = c_{12}\alpha_1 + (c_{22} + c_{23})\alpha_2 \quad (1e)$$

and

$$U = u/b, \qquad V = v/b, \qquad R = r/b \quad (1f)$$

In Eqs. (1), the c_{ij} are elastic constants‡; α_1 and α_2 are coefficients of thermal expansion in the radial and circumferential directions, respectively; T is the temperature measured relative to an ambient temperature at which the body is stress free; u, v are the radial and circumferential components of displacements, respectively. Equilibrium requires that the dimensionless displacement components U and V satisfy the system of equations

$$c_{11}\frac{\partial^2 U}{\partial R^2} + \frac{c_{44}}{R^2}\frac{\partial^2 U}{\partial\theta^2} + \frac{c_{11}}{R}\frac{\partial U}{\partial R} - \frac{c_{22}}{R^2}U + \frac{(c_{12}+c_{44})}{R}\frac{\partial^2 V}{\partial R\partial\theta} - \frac{(c_{22}+c_{44})}{R^2}\frac{\partial V}{\partial\theta} = \lambda_1\frac{\partial T}{\partial R} + \frac{(\lambda_1-\lambda_2)}{R}T \quad (2a)$$

$$c_{44}\frac{\partial^2 V}{\partial R^2} + \frac{c_{22}}{R^2}\frac{\partial^2 V}{\partial\theta^2} + \frac{c_{44}}{R}\frac{\partial V}{\partial R} - \frac{c_{44}}{R^2}V + \frac{(c_{12}+c_{44})}{R}\frac{\partial^2 U}{\partial R\partial\theta} + \frac{(c_{22}+c_{44})}{R^2}\frac{\partial U}{\partial\theta} = \frac{\lambda_2}{R}\frac{\partial T}{\partial\theta} \quad (2b)$$

for some prescribed temperature T. For this problem, T will be assumed symmetric about $\theta = 0$ and to be expressible in the form

$$T(R,\theta) = \sum_{n=0}^{\infty}\sum_{m=0}^{\infty} T_{nm}R^m \cos n\theta \quad (3)$$

The stress and displacement fields associated with this particular form of the temperature T have representations

$$U = \sum_{n=0}^{\infty} U_n(R)\cos n\theta, \qquad V = \sum_{n=1}^{\infty} V_n(R)\sin n\theta \quad (4a)$$

$$\sigma_r = \sum_{n=0}^{\infty} S_r{}^n(R)\cos n\theta, \qquad \sigma_\theta = \sum_{n=0}^{\infty} S_\theta{}^n(R)\cos n\theta$$

$$\tau_{r\theta} = \sum_{n=1}^{\infty} S_{r\theta}{}^n(R)\sin n\theta \quad (4b)$$

Stress Formulas

Expressions will now be developed for the R-dependent terms $U_n(R)$, $V_n(R)$, $S_r{}^n(R)$, $S_\theta{}^n(R)$, and $S_{r\theta}{}^n(R)$ of Eqs. (4). In order to circumvent certain degeneracies which occur in the field Eqs. (2) for $n = 0,1$, these values of n will be considered separately from the general case $n \geq 2$.

Received May 26, 1969; revision received July 9, 1969. This work was supported by the U.S. Atomic Energy Commission.

* Staff Member.

† Staff Member. Member AIAA.

‡ Relationships between the c_{ij} and Young's moduli and Poisson's ratios are given in Ref. 4.